PECULIARITIES OF ULF WAVE CHARACTERISTICS
IN A MULTICOMPONENT IONOSPHERIC PLASMA

D.S. Kotik (iD)
Radiophysical Research Institute,
Nizhny Novgorod, Russia, dmitry.kotik@nirfi.unn.ru

E.V. Orlova (iD)
N.I. Lobachevsky State University of Nizhny Novgorod,
Nizhny Novgorod, Russia, ekaterina.orlova.94@bk.ru

V.A. Yashnov (iD)
N.I. Lobachevsky State University of Nizhny Novgorod,
Nizhny Novgorod, Russia, vay@rf.unn.ru

Abstract. We have examined the properties of low-frequency electromagnetic waves in multicomponent ionospheric plasma in the 1–30 Hz band, using the magnetoionic theory. Complex permittivity tensor components and refractive indices of normal waves (ordinary and extraordinary) were calculated at altitudes from 80 to 750 km. The calculations show that the refractive indices are highly dependent on frequency and height. Polarization of ordinary and extraordinary waves is elliptical over the entire range of the frequencies investigated. The refractive index and the polarization of normal waves are demonstrated to tend to magnetohydrodynamic (MHD) values only at frequencies lower than 1 Hz. The group velocity vector of an extraordinary wave is not directed along the magnetic field, as follows from the MHD approximation, but it lies inside a cone within ±(5–10) degrees, depending on frequency. The group velocity vector of an ordinary wave is practically independent of the angle with the geomagnetic field as in the MHD approximation. The proposed method for calculating the characteristics of normal waves in the ionosphere can be used to study ULF wave propagation from both natural and artificial ionospheric sources, which arise under the action of powerful HF radio waves in the lower and upper ionosphere.

Keywords: ULF waves, ionosphere, refractive index, polarization, Alfvén wave, fast magnetosonic wave.

INTRODUCTION

Since the first publications [Jacobs, Watanabe, 1962; Greifinger, Greifinger, 1968], ULF wave propagation in ionospheric plasma has been traditionally investigated in the framework of magnetohydrodynamics (MHD) in terms of Alfvén (A) and fast magnetosonic (FMS) waves. This approximation is still used quite often today when studying properties of the ionospheric MHD waveguide [Fujita, 1987, 1988] or the ionospheric Alfvén resonator (IAR) (see, e.g., [Polyakov, Rapoport, 1981; Lysak et al., 2013]). Starting with one of the first works [Ginzburg, 1963], the magnetoionic theory has generally been applied to dispersion properties of ionospheric plasma in ion gyrofrequencies. These are the so-called problems of crossover and ion whistlers (see, e.g., [Singh et al., 2002; Vavilov, Shklyar, 2016]). In some papers, the multicomponent plasma model has been considered in connection with particular issues. So, Aydogdu and Ozca [1996] studied the influence of inclination of the magnetic field on the refractive index (our algorithm makes this automatically); and Yeşil and Sağir [2019] compared the conductivity tensor for cold and warm plasma in the F layer of the equatorial ionosphere.

We think it is important and topical to take into account the properties of normal waves in the problems of ULF wave propagation in the MHD waveguide, as well as in the problems of arrival of ULF waves at Earth and their penetration into the magnetosphere since the coefficients of reflection, refraction, and transformation of normal waves at boundaries of ionospheric layers (boundary conditions) depend on polarization of normal waves. We have employed the proposed algorithm to calculate propagation paths of ULF waves [Kotik et al., 2021], generated in the upper ionosphere by the HAARP facility [Eliasson et al., 2012], and propagation of signals from ionospheric or terrestrial ULF source in the Earth—ionosphere waveguide [Ermakova et al., 2022]. This method was also used to study the effect of geomagnetic activity variations on polarization spectra of low-frequency magnetic noise in the ULF range [Ermakova et al., 2021]. Applying the magnetoionic theory to the ULF range is also essential for quantitative simulation of spectral characteristics of the ionospheric Alfvén resonator (see, e.g., [Ermakova et al., 2007]) and for interpretation of properties of natural geomagnetic pulsations [Ermakova et al., 2019].

The algorithm described in this paper for calculating the refractive index in the ionospheric model close to reality has proved valid in modeling and interpreting the dynamics of IAR spectra under various conditions and ULF-wave propagation effects (examples are given in the above and other works of co-authors).

By "simulation has been carried out" is generally meant a lot of work on developing an algorithm and a program code, which yields certain results, usually presented as plots. The purpose of this paper is to present our algorithm explicitly so that anyone can use it for their own research. Besides, we have made sure that the results of our studies into the properties of ULF waves in the ionosphere

based on the magnetoionic theory have independent significance and have not been published by anyone before. The main characteristics of ULF waves in the ionosphere calculated by this algorithm differ significantly from those obtained in the MHD approximation, which should be taken into account when numerically simulating ULF-wave radiation and propagation, as well as when interpreting the results of experiments on ionospheric generation of ULF waves by powerful HF radio radiation [Kotik et al., 2013].

In this paper, the properties of ULF waves in ionospheric plasma are studied in detail using the magnetoionic theory and international models of ionosphere IRI-2016, atmosphere MSIS-E-90, and geomagnetic field DGRF/IGRF. We calculate the altitude dependences of complex permittivity tensor components, collision frequency, refractive indices, and polarization of normal waves in ULF. Features of group velocity and surfaces of wave normals are analyzed. The results we present demonstrate a significant difference from those obtained in the MHD approximation.

The properties of normal waves in the ionospheric F-region become similar to those of A-waves and FMS waves only at frequencies lower than 1 Hz (or at altitudes around 800–1000 km and higher for higher frequencies). In what follows, we arbitrarily call one of the normal (extraordinary) waves the A-wave; and the ordinary one, the FMS wave.

1. BASIC EQUATIONS

Components of the complex permittivity tensor of magnetoactive plasma are calculated from a system of charged and neutral particle motion equations. The expression for the molecular velocity $\vec{v}_\mathrm{m}$ in the lower ionosphere can be derived from system of equations (10.34)–(10.36) for motion of electrons, ions, and neutral particles, given in the monograph [Ginzburg, 1963]:

$$\vec{v}_\mathrm{m} = \left(\frac{mN_\mathrm{e}}{MN_\mathrm{m}} \nu_\mathrm{em} \left(\vec{v}_\mathrm{e} - \vec{v}_\mathrm{i} \right) + \frac{N_\mathrm{e}}{N_\mathrm{m}} \vec{v}_\mathrm{im} \left(\vec{v}_\mathrm{m} - \vec{v}_\mathrm{i} \right) \right) \times$$

$$\times \left(-i\omega + \nu_\mathrm{im} \frac{N_\mathrm{e}}{N_\mathrm{m}} \right)^{-1}, \tag{1}$$

where m, M are electron and ion masses; N_e, N_m are electron and neutral particle concentrations; $\vec{v}_\mathrm{e}$, $\vec{v}_\mathrm{i}$ are electron and ion velocities; ν_em, ν_im are frequencies of collisions of electrons and ions with neutral particles; $\omega = 2\pi f$ is the angular wave frequency. In the lower ionosphere, the inequality $\omega \gg \nu_\mathrm{im} N_\mathrm{e} / N_\mathrm{m}$ holds for frequencies higher than 0.01 Hz by a wide margin up to $\sim 10^{-5}$. This makes it possible to exclude the terms with molecular velocity from (10.34). Neglecting the terms of the order of (m/M), $\sqrt{m/M}$, in view of the inequality $\nu_\mathrm{im} \ll \nu_\mathrm{em} \sqrt{m/M}$, the system of electron and ion motion equations for a multicomponent plasma can be simplified as follows

$$\left(-i\omega + \nu_\mathrm{em} + \nu_\mathrm{ei} \right) v_\mathrm{e} = \frac{e}{m} \vec{E} + \frac{e}{mc} \left[\vec{v}_\mathrm{e}, \vec{H}_0 \right], \tag{2}$$

$$\left(-i\omega + \nu_\mathrm{km} \right) \vec{v}_\mathrm{k} = -\frac{e}{m_\mathrm{k}} \vec{E} + \frac{e}{m_\mathrm{k} c} \left[\vec{v}_\mathrm{k}, \vec{H}_0 \right], \tag{3}$$

where k is the type of charged particle (electrons and ions); m_k is the particle mass; ν_km is the frequency of collisions of k-th type particle with molecules and ions; c is the speed of light in vacuum; e is the electron charge; $\vec{H}_0$ is the geomagnetic field strength.

The permittivity tensor in ULF in a coordinate system with Z axis directed along the magnetic field can be derived from (2), (3):

$$\varepsilon_{xx} = \varepsilon_{yy} = \varepsilon_1 =$$

$$= 1 - \frac{1}{2} \sum_{k=1}^{K} \frac{\omega_\mathrm{pk}^2}{\omega} \left(\frac{1}{\omega - i\nu_\mathrm{k} - \omega_\mathrm{Hk}} + \frac{1}{\omega - i\nu_\mathrm{k} + \omega_\mathrm{Hk}} \right),$$

$$\varepsilon_{xy} = \varepsilon_{yx} = -i\varepsilon_2 =$$

$$= -i\frac{1}{2} \sum_{k=1}^{K} \frac{\omega_\mathrm{pk}^2}{\omega} \left(\frac{1}{\omega - i\nu_\mathrm{k} - \omega_\mathrm{Hk}} - \frac{1}{\omega - i\nu_\mathrm{k} + \omega_\mathrm{Hk}} \right), \tag{4}$$

$$\varepsilon_{zz} = \varepsilon_3 = 1 - \sum_{k=1}^{K} \frac{\omega_\mathrm{pk}^2}{\omega\left(\omega - i\nu_\mathrm{k} \right)}.$$

Here, $\omega_\mathrm{Hk} = \pm eH_0 / \left(m_\mathrm{k} c \right)$ are gyrofrequencies of electrons (–) and ions (+); $\omega_\mathrm{pk} = \left(4\pi e^2 N_\mathrm{k} / m_\mathrm{k} \right)$ are plasma frequencies of the k-th type particles; ν_k are the effective collision frequencies, which are the sum of the frequencies of collisions with ions and neutral particles of all types.

The frequencies of collisions of electrons and ions with plasma particles have been calculated using formulas from [Fatkullin et al., 1981].

The total frequency of collisions of electrons with positive ions of all types is determined from the formula

$$\nu_\mathrm{ei} = 54 \cdot 10^{-9} N_\mathrm{e} / T_\mathrm{e}^{3/2}. \tag{5}$$

Here N_e, T_e are the electron density and temperature respectively.

The frequencies of collisions of electrons with molecules (molecular and atomic oxygen O_2 and O, nitrogen N_2, atomic hydrogen H, helium He) were calculated from the following formulas:

$$\nu\left(e, O_2 \right) = 1.82 \cdot 10^{-10} n\left(O_2 \right) \times$$

$$\times \left(1 + 3.6 \cdot 10^{-2} T_\mathrm{e}^{1/2} \right),$$

$$\nu\left(e, N_2 \right) = 2.33 \cdot 10^{-11} n\left(N_2 \right) \times$$

$$\times \left(1 - 1.21 \cdot 10^{-4} T_\mathrm{e} \right) T_\mathrm{e},$$

$$\nu\left(e, O \right) = 2.8 \cdot 10^{-10} n\left(O \right) T_\mathrm{e}^{1/2}, \tag{6}$$

$$\nu\left(e, H \right) = 4.5 \cdot 10^{-9} n\left(H \right) \left(1 - 1.35 \cdot 10^{-4} T_\mathrm{e} \right) T_\mathrm{e}^{1/2},$$

$$\nu\left(e, He \right) = 4.6 \cdot 10^{-10} n\left(He \right) T_\mathrm{e}^{1/2},$$

$$\nu_\mathrm{em} = \sum_{k=1}^{5} \nu_\mathrm{ek}.$$

The total effective frequency of electron collisions $\nu_e = \nu_{em} + \nu_{ei}$.

The frequencies of collisions of ions O_2^+ with molecules were calculated from the formulas

$$\nu\left(O_2^+, O_2\right) = 1.17 \cdot 10^{-9} n\left(O_2\right)\left(\frac{T_i + T_n}{2000}\right)^{0.28},$$

$$\nu\left(O_2^+, O, N_2\right) = \left(0.75 n(O) + 0.89 n(N_2)\right)^{-9},$$

$$\nu_{O_2^+ m} = \nu\left(O_2^+, O_2\right) + \nu\left(O_2^+, O, N_2\right). \tag{7}$$

The frequency of collisions of NO+ with molecules was computed from the formula

$$\nu_{NO^+ m} =$$
$$= \left(0.83 n(O_2) + 0.76 n(NO) + 0.76 n(N_2)\right)10^{-9}. \tag{8}$$

For the frequency of collisions of O^+ with molecules

$$\nu_{O^+ m} = \left(n(NO + 1.08 n(N_2))\right)10^{-9}. \tag{9}$$

In Formulas (6)–(9), $n\left(X_k\right)$ and $n\left(Y_k^+\right)$ are concentrations of neutral particles and ions of all types in the ionosphere. In Formula (9), collisions with O_2 are ignored. Similarly, formulas from [Fatkullin et al., 1981] were also used to calculate the frequencies of collisions of ions of various types with other charged particles.

It is convenient to represent the refractive indices of normal waves in ionospheric plasma at an arbitrary angle θ between geomagnetic field direction and wave vector (the Z axis is directed to the zenith) as follows [Helliwell, 1965]:

$$\left(n - i\kappa\right)_{1,2}^2 = \frac{L \pm \sqrt{R}}{D}, \tag{10}$$

$$L = (\varepsilon_{xx}^2 + \varepsilon_{yy}^2)\sin^2\theta + \varepsilon_{xx}\varepsilon_{zz}(1 + \cos^2\theta),$$
$$D = 2(\varepsilon_{xx}\sin^2\theta + \varepsilon_{zz}\cos^2\theta), \tag{11}$$
$$R = L^2 - 2D(\varepsilon_{xx}^2 + \varepsilon_{xy}^2)\varepsilon_{zz}.$$

Expression (10) is significantly simplified in the special case of propagation along the magnetic field and becomes (12), where 1 and 2 correspond to two normal modes in the ionosphere:

$$\left(n - i\kappa\right)_{1,2} = \sqrt{\varepsilon_{xx} \pm i\varepsilon_{xy}}. \tag{12}$$

It is also easy to show that in the lower ionosphere in the E layer, where ions can be considered nonmagnetized, the real part of the refractive index of one of the normal waves coincides with the index of the whistler mode (the wave has circular polarization) and the expression for the refractive index of a vertically propagating wave is given by the formula

$$n^2 = \frac{\omega_{pe}^2}{\omega_{H(NO^+)}\omega\cos\theta}. \tag{13}$$

It is assumed here that in the E layer, NO^+ is the dominant ion (this follows from IRI-2016, see Figure 1, *a*). At altitudes above 150 km, the refractive index of ordinary wave n_1 is close to the refractive index of FMS wave, and that of extraordinary wave n_2 is close to the refractive index of A-wave, corrected for the closeness of the wave frequency to the ionic gyrofrequency:

$$n_1 = \frac{\omega_{0i}}{\omega_{Hi}}\left(1 + \frac{\omega^2}{\omega_{Hi}^2}\right), \quad n_2 = n_1\cos\theta, \tag{14}$$

where i is the type of dominant ion at a given height.

In the limit when the wave frequency $\omega \to 0$, the first of the normal waves (ordinary O) becomes an FMS wave; and the second (extraordinary EO), an A-wave. Formulas (13) and (14) are convenient to use for estimates. In this paper, we apply Formulas (4)–(11) to the characteristics of normal waves. For convenience, we will call them FMS and A-waves.

The dispersion equation for normal waves in a cold magnetoactive plasma can be written as follows (see, e.g., [Ginzburg, Rukhadze, 1972]):

$$F \equiv \frac{1}{2}\left[k^2 - \frac{\omega^2}{c^2}n^2\left(\omega, \theta\right)\right] = 0, \tag{15}$$

where $\vec{k}$ is the wave vector; $n(\omega,\theta)$ is the wave refractive index determined by Equation (15).

The group velocity can be calculated with the formula

$$\vec{V}_g = -\left(\frac{\partial F}{\partial \vec{k}}\right)\Big/\left(\frac{\partial F}{\partial \omega}\right). \tag{16}$$
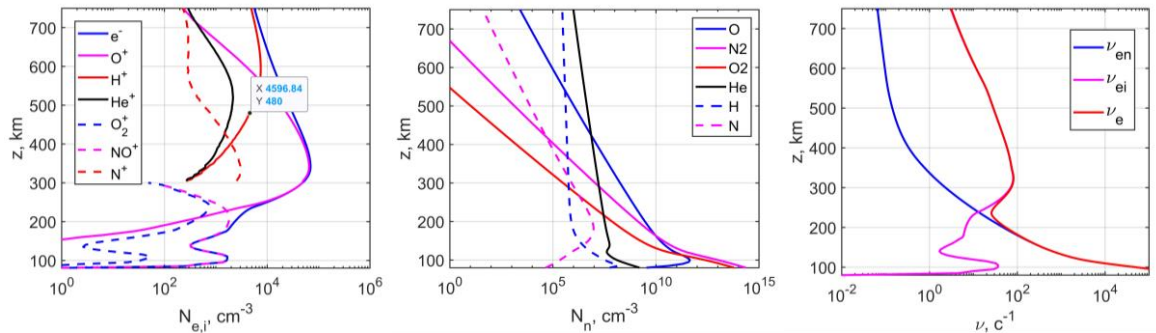
Figure 1. Vertical profiles: electron and ion concentrations (cm^{-3}) (*a*); neutral molecule concentration (cm^{-3}) (*b*); calculated frequencies of electron collisions with neutral particle and ions, and the sum of the last two values (c^{-3}) (*c*). Winter, midlatitudes, midnight

It is assumed here that the external magnetic field is directed along the Z axis, and the wave vector lies in the XZ plane and makes an angle θ with the direction of the geomagnetic field. In this case,

$$n^2(\omega, \theta) = n^2(\omega, \cos\theta), \quad \cos\theta = k_z / \sqrt{k_x^2 + k_z^2}.$$

2. IONOSPHERIC MODEL

The upper atmosphere parameters have been obtained using the international models of charged and neutral particles and the geomagnetic field (see Introduction and Section 5). The calculations were mainly carried out for the mid-latitude ionosphere. For certainty, we took a point with geographic coordinates 59° N, 46° E, corresponding to the position of the SURA facility. We present the results of calculations for winter (January 1) and summer (July 1). These models are used in most of the subsequent calculations, unless otherwise indicated.

Figure 1 exemplifies the profiles of neutral (*a*) and charged (*b*) particles in ionospheric plasma, as well as the altitude dependence of the frequency of collisions of electrons with neutral particles and ions (*c*), calculated from Formulas (5)–(9).

3. RESULTS

3.1. Permittivity tensor and refractive index of ULF waves

Figure 2 exemplifies the calculation of complex permittivity tensor components for given dates and coordinates from Formulas (4).

The tensor components are seen to strongly depend on the time of day. Of particular note is the tensor component ε$_{xy}$ responsible for the gyrotropy of the medium. This component differs markedly from zero to the heights of the outer ionosphere. Recall that in the MHD approximation the gyrotropic component of the medium conductivity tensor is zero.

Figure 3 presents the result of calculation of altitude dependences of the ULF wave refractive index for three frequencies from Formulas (2)–(10). There, for comparison, a similar dependence obtained in the MHD approximation is given (black curve). The real and imaginary parts of the refractive and absorption indices of both normal modes strongly depend on frequency. At frequencies of 10 and 20 Hz, they differ significantly from the MHD values in both the lower and upper ionosphere. At a frequency of 1 Hz and below, the A-wave real part coincides with the refractive index of the A-wave calculated in the MHD approximation at altitudes above 200 km. There is a significant difference in the lower ionosphere.

The main feature of the above profiles of the real and imaginary parts of the refractive indices is a strong frequency dependence.

It is also obvious that the magnetoionic theory yields adequate values for the imaginary parts of the refractive index, which also depend greatly on frequency. The A-wave is seen to experience strong attenuation in the lower ionosphere, whereas the FMS wave is subject to weak attenuation, and the real part of its refractive index acquires a characteristic whistler shape.

Figure 4 shows the profiles of refractive indices of ULF waves for winter and summer and their day-to-night variations.

During the transition from winter to summer, the refractive index is seen to change approximately twice, whereas its daily variation is within 4–5.

Figure 5 shows the latitude dependence of the refractive index of ULF waves, using three known heating facilities as an example.

It can be seen that the difference between the middle and high latitudes is insignificant. For low (subequatorial) latitudes, the refractive indices may differ 3–4 times from those for middle latitudes.

3.2 Attenuation of ULF waves

Propagation of ULF waves in the ionospheric MHD waveguide at frequencies below 3–4 Hz is described in the mode approximation (see the works cited in Introduction). However, at higher frequencies, when the transverse size of the waveguide is larger than the wavelength in the medium, it is possible to switch to geometrical optics (see [Whang, 1997; Kotik et al., 2021]). In particular, given the imaginary part of the refractive index, it is easy to calculate the azimuth angle φ and frequency dependence of the absorption coefficient of MHD waves in the ionosphere. Examples of the azimuthal dependence are presented in Figure 6.
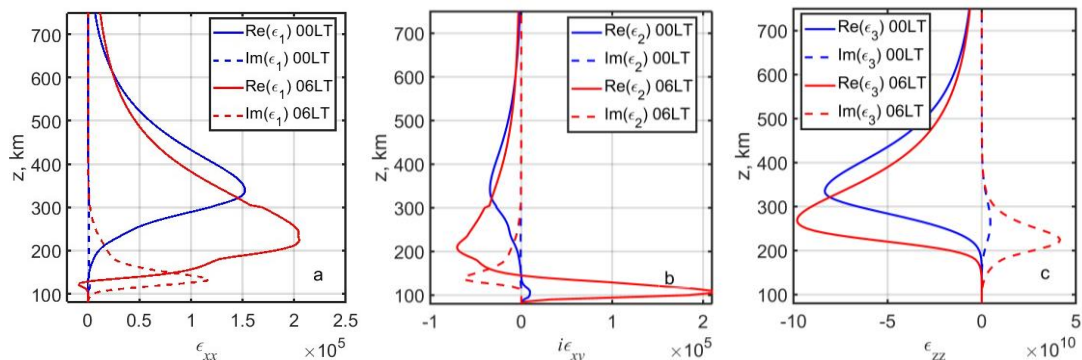
Figure 2. Profiles of complex permittivity tensor components for morning (red curve) and midnight (blue curve), *f*=10 Hz
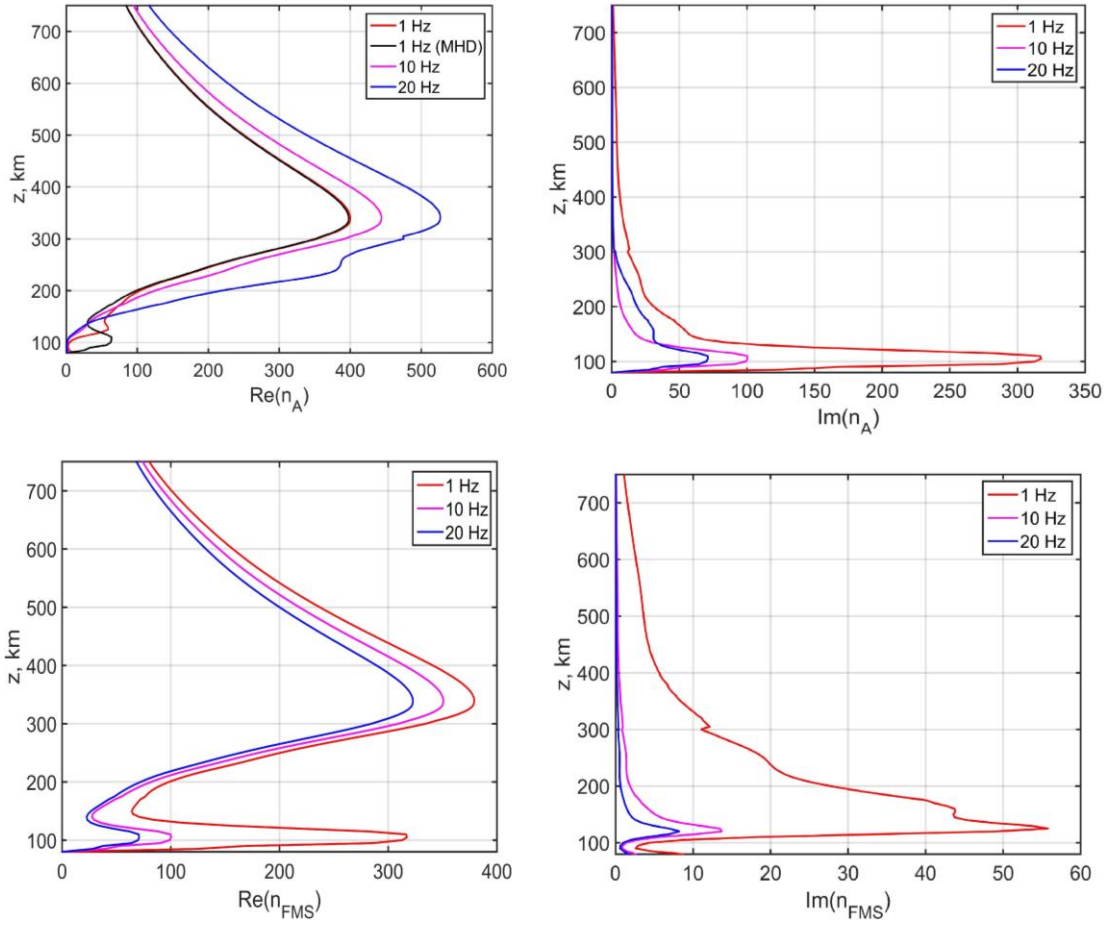
Figure. 3. Vertical profiles of real and imaginary parts of refractive indices of normal waves: for A-wave (top panel), for FMS wave (bottom panel)
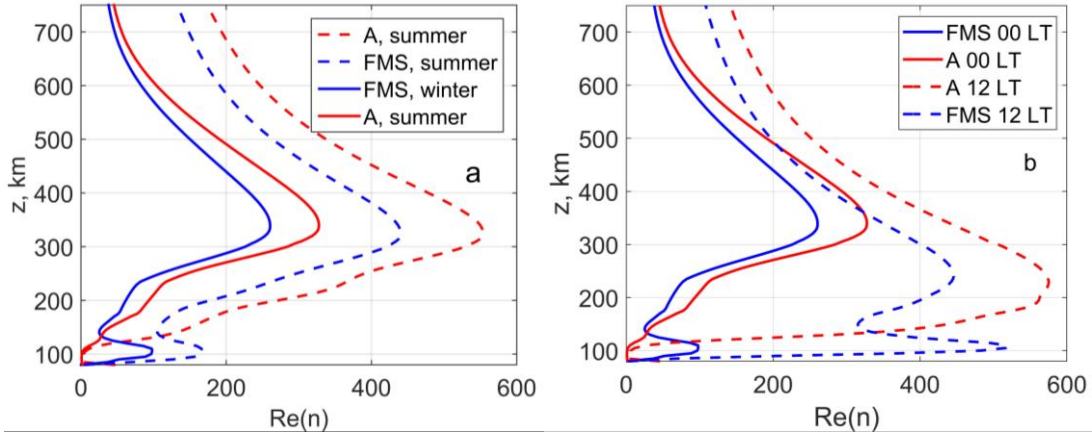
Figure 4. Seasonal variations in vertical profiles of refractive indices of ULF waves for a frequency of 10 Hz (left) versus the diurnal variation (right) at midlatitudes

It can be seen that the A-wave in the MHD wave-guide attenuates much more strongly than the FMS wave whose damping is essentially independent of propagation direction. This fact is consistent with the experimentally observed simultaneous recording of pulsations at stations widely spaced in latitude [Ermakova et al., 2019], as well as with the experiments on recording artificial signals, generated in the ionosphere by the HAARP facility, at a network of stations in the Pacific Ocean in the 1–40 Hz range [Eliasson et al., 2012].

3.3 Polarization of ULF waves in the ionosphere

We characterize the ULF-wave polarization degree by $P = \left| E_x / E_y \right| \exp(i\Delta\phi)$, where $\Delta\phi$ is the phase shift between E_x and E_y. Wave polarization becomes elliptical when $\Delta\phi = \pm\pi / 2$. Figure 7 shows the polarization dependence on frequency (0.1, 1, and 10 Hz) for the ionospheric E- and F- regions.
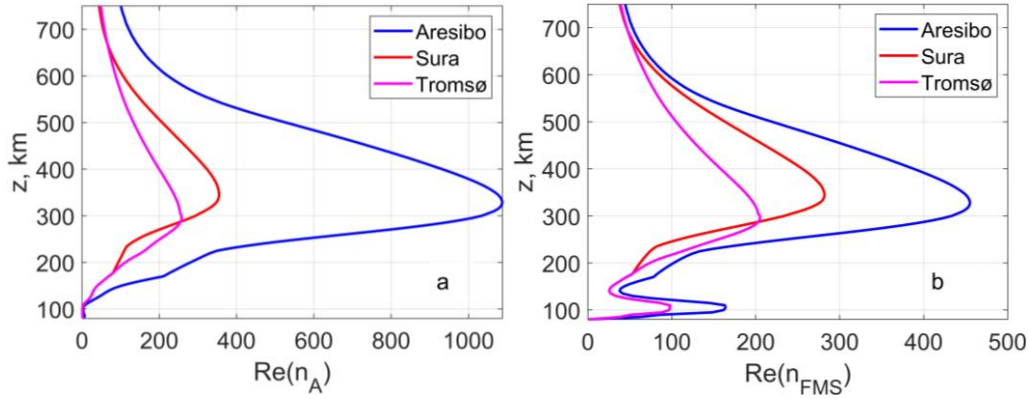
Figure 5. Profiles of the real part of refractive indices of ULF waves for different latitudes (winter, midnight)
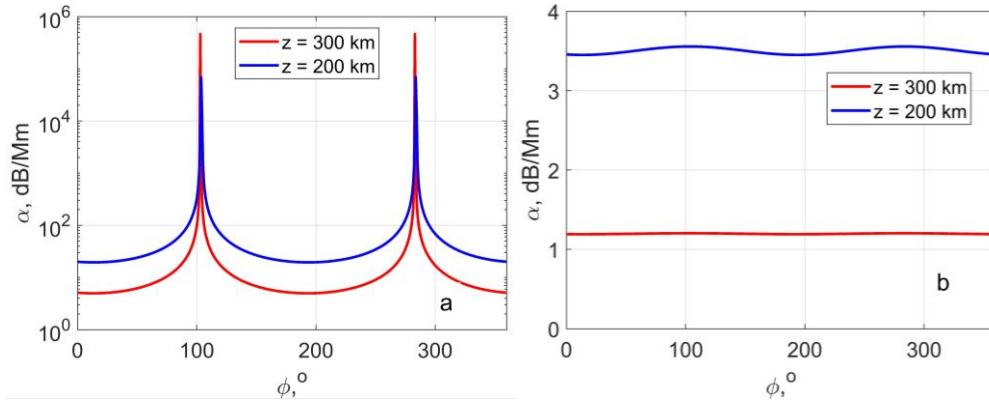
Figure 6. Attenuation coefficients as function of the azimuthal direction of propagation for a frequency of 10 Hz at altitudes of 200 and 300 km: A-wave (*a*), FMS wave (*b*)
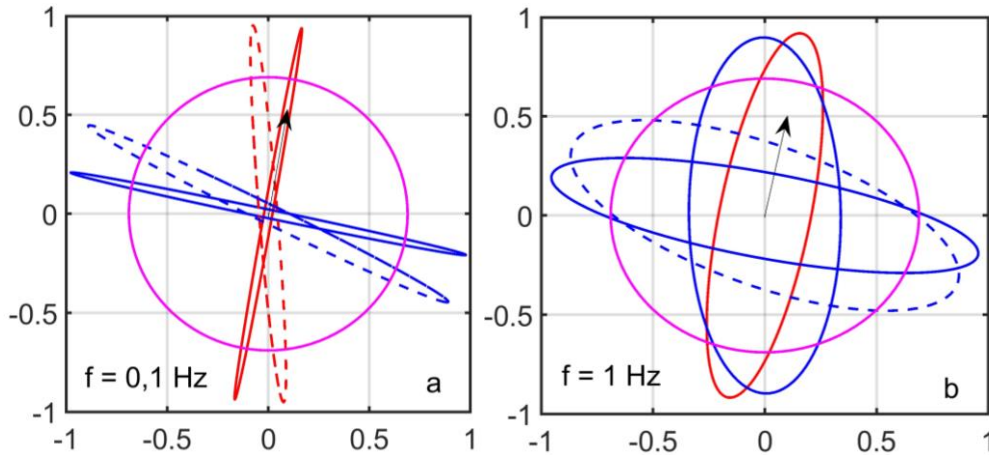
Figure 7. Polarization properties of ELF waves for three frequencies and three given heights (300 km — solid lines, 200 km — dotted lines, 100 km — pink line for the whistler mode). The blue color marks an FMS wave; the red color, an A-wave. The black arrow is a projection of the geomagnetic field on a horizontal plane

The ULF-wave polarization in the ionosphere is seen to be very different from that in the MHD approximation, which, as is well known, is linear and frequency-independent [Alfvén, 1952]. The polarization becomes almost linear for frequencies below 0.1 Hz in the F-region and above. For frequencies of ~1 Hz, the polarization turns out to be elliptical, and for frequencies of 10 Hz and higher, it is almost circular. In the E-region, where the refractive index is close to the whistler one, polarization becomes almost circular.

3.4. Group velocity of ULF waves in the ionosphere

The θ angle dependences of the group velocity vector direction (angle α) and the shape of wave normal surfaces for ULF waves, calculated from Formulas (15)–(17) for two frequencies, are shown in Figure 8 for 350 and 110 km. Recall that the group velocity vector is perpendicular to the wave normal surface. It can be seen that in the F-region and above, the deviation of the group velocity vector from the direction of the geomagnetic field does
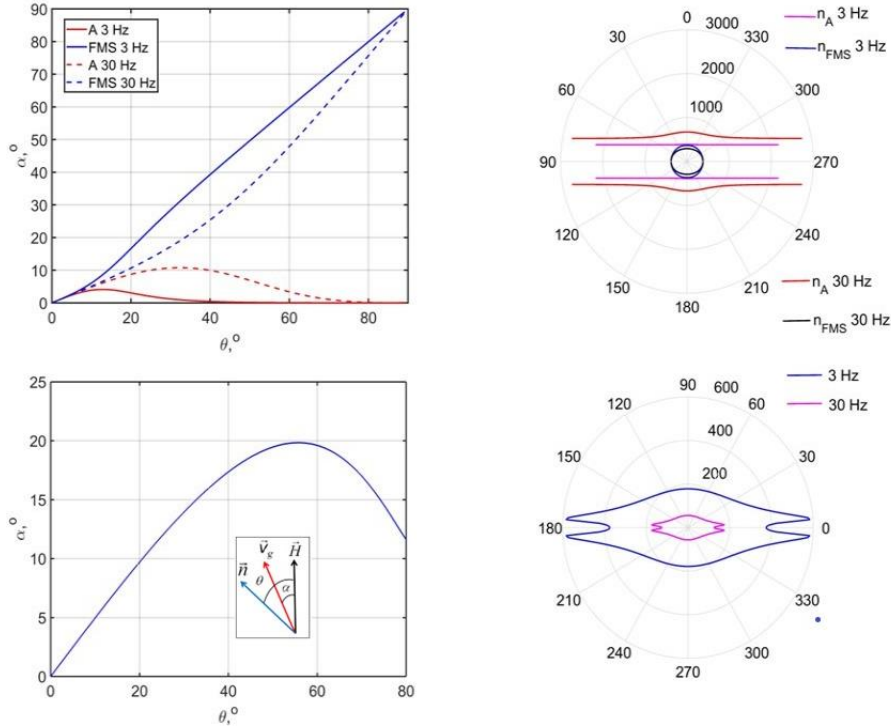
Figure 8. Group velocity vector direction (angle α) versus wave normal direction (angle θ): 350 km (*a*), 110 km (*b*); and shape of wave normal surfaces: 350 km (*c*),110 km (*d*) for 3 and 30 Hz frequencies

not exceed 5° for a frequency of 3 Hz and 10° for a frequency of 30 Hz. The FMS wave propagates almost isotropically at all altitudes, as with the MHD approach. It can also be seen that for a frequency of 3 Hz and below the wave normal surfaces are close to those in the MHD approximation [Alfvén, 1952], but they differ markedly for a frequency of 30 Hz and higher in the F layer.

In the E layer, the dependence of the group velocity vector direction (panel *b*) and the wave normal surface (*d*) in the ULF range differ significantly from both the MHD approximation and the VLF whistler mode, despite the fact that the refractive index is close to the whistler one (Story's theorem, [Helliwell, 1965]).

4.   DISCUSSION

The results of our studies into the properties of ULF waves within 0.3–30 Hz in a multicomponent ionospheric plasma based on the magnetoionic theory have shown a significant difference from the results following from the MHD approximation.

1. Values of the real part of the refractive index of normal waves in the F-region are 1.5–2 times higher than those predicted by the MHD theory. In the E-region, the gyrotropy effect is significant; therefore, the refractive index of one of the normal modes (FMS) becomes close to the whistler mode with circular polarization, and the second mode is strongly attenuated (see Figures 1, 2). The refractive index values themselves depend greatly on the time of day, season, and latitude (see Figures 3–5).

2. FMS waves are weakly attenuated when propagating in any directions both in the MHD waveguide and in the magnetosphere. This statement is confirmed by experiments with artificial ionospheric source [Eliasson et al., 2012] and by observations of natural magnetic pulsations at mid-latitude stations spaced in longitude by 45° [Ermakova et al., 2019]. For A-waves, the attenuation increases significantly when they propagate across the magnetic field — it is much higher than for FMS waves (see Figure 6).

3. Polarization of normal waves over the entire frequency range and at all altitudes of the ionosphere is generally elliptical. Polarization for all ULF frequencies becomes almost linear, and the orientation of the main axes of the ellipse coincides with the orientation of A-waves and FMS waves only in the outer ionosphere at altitudes over 600 km. At frequencies below 0.1 Hz, polarization is close to the case of the MHD approximation already in the F layer (see Figure 7).

4. Direction of the group velocity vector of normal waves is also very different from that predicted in the framework of the MHD approximation. The A-wave propagates in a cone with an axis along the magnetic field, the opening of which depends on frequency, being as wide as 10° at a frequency of 30 Hz. At the same time, the magnetic field does not have a directive effect on the FMS wave.

Applying the magnetoionic theory to the ULF range is essential for quantitative simulation of spectral characteristics of the ionospheric Alfvén resonator and for interpretation of properties of natural geomagnetic pulsations (see, e.g., [Ermakova et al., 2007, 2019]).

5.   STATEMENT ON DATA AVAILABILITY

When selecting data for given coordinates and time, we have used models calculated from the codes available at:

- [https://ccmc.gsfc.nasa.gov/modelweb/models/iri2016_vitmo.php] for the electron density from IRI-2016;
- [https://ccmc.gsfc.nasa.gov/modelweb/models/msis_vitmo.php] for the atmospheric layer density from MSIS-E-00;
- [https://ccmc.gsfc.nasa.gov/modelweb/models/igrf_vitmo.php] for the geomagnetic field from DGRF/IGRF.

The above codes were embedded in the main code for calculating the refractive index of normal waves in the ionosphere.

REFERENCES

Alfvén H. *Cosmical Electrodynamics*. Oxford, Clarendon Press, 1950. 237 p.

Aydogdu M., Ozca O. Effect of magnetic declination on refractive index and wave polarization coefficients of electromagnetic waves in mid-latitude ionosphere. *Indian J. Radio and Space Phys*. 1996, vol. 25, pp. 263–270.

Eliasson B., Chang C.-L., Papadopoulos K. Generation of ELF and ULF electromagnetic waves by modulated heating of the ionospheric F2 region. *J. Geophys. Res*. 2012, vol. 117, no. A10320. DOI: 10.1029/2012JA017935.

Ermakova E.N., Kotik D.S., Polyakov S.V., Shchennikov A.V. On a mechanism forming a broadband maximum in the spectrum of background noise at frequencies 2–6 Hz. *Radiophysics and Quantum Electronics*. 2007, vol. 50, no. 7, pp. 555–569. DOI: 10.1007/s11141-007-0049.

Ermakova E.N., Demekhov A.G., Yahnina T., et al. Dynamics of the spectra of multiband Pc1 pulsations in the presence of multiple regions of ion–cyclotron instability in the magnetosphere. *Radiophysics and Quantum Electronics*. 2019, vol. 62, no.7. DOI: 10.1007/s11141-019-09950-5.

Ermakova E.N., Ryabov A.V., Kotik D.S. Influence of geomagnetic activity variations on polarization spectra of ULF magnetic noise based on ground-based monitoring data. Proc. XXVII All-Russian Open Scientific Conference "Propagation of Radio Waves". Kaliningrad, 2021, pp. 269–274.

Ermakova E.N., Kotik D.S., Ryabov A.V. Characteristics of ULF magnetic fields in the 3D inhomogeneous Earth — ionosphere waveguide. *J. Geophys. Res.: Space Phys*. 2022, vol. 127, no. 3. DOI: 10.1029/2021JA030025.

Fatkullin M.N., Zelenova T.I., Kozlov V.K., Legen'ka D., Soboleva T.N. Empirical Models of the Mid-Latitude Ionosphere. Moscow, Nauka Publ., 1981. 256 p. (In Russian).

Fujita S. Duct propagation of a short-period hydromagnetic wave based on the international reference ionosphere model. *Planetary Space Sci*. 1987, vol. 35, no. 91, pp. 91–103. DOI: 10.1016/0032-0633(87)90148-6.

Fujita S. Duct propagation of hydromagnetic waves in the upper ionosphere. Dispersion characteristics and loss mechanism. *J. Geophys. Res*. 1988, vol. 93, no. A12, pp. 14674–14682. DOI: 10.1029/JA093iA12p14674.

Ginzburg V.L. *The Propagation of Electromagnetic Waves in Plasmas*. Oxford, NewYork, Pergamon Press, 1970, 615 p.

Ginzburg V.L., Rukhadze A.A. *Waves in Magnetoplasma*. Handbook Elektrophys. Springer Verlag, 1972. 216 p.

Gintzburg M. A. Low-frequency waves in multicomponent plasma. *Geomagnetism and Aeronomy*. 1963, no.3, pp. 610–614, (In Russian).

Greifinger C., Greifinger S. Theory of hydromagnetic propagation in the ionospheric waveguide. *J. Geophys. Res*. 1968, vol. 73, no. 23. pp. 7473–7490.

Helliwell R. *Whistlers and Related Ionospheric Phenomena*. Stanford University Press, 1965.

Jacobs J.A., Watanabe T. Propagation of hydromagnetic waves in the lower exosphere and the origin of short period geomagnetic pulsations. *J. Atmos. Terr. Phys*. 1962, vol. 24, pp. 413–419.

Kotik D.S., A.V. Ryabov, E.N. Ermakova et al. Properties of the ULF/VLF !!?signals generated by the SURA facility in the upper ionosphere. *Radiophysics and Quantum Electronics*. 2013, vol. 56, no. 6. pp. 344–354. DOI: 10.1007/s11141-013-9438-9.

Kotik D.S., Ryabov A.V., Yashnov V.A., Orlova E.V. Propagation of ULF radiation from an artificial ionospheric source in a 3D inhomogeneous MHD waveguide. *Radiophysics and Quantum Electronics*. 2021, vol. 64, no. 1, pp. 1–10. DOI: 10.1007/s11141-021-10107-6.

Lysak R.L., Waters C.L., Sciffer M.D. Modeling of the ionospheric Alfvén resonator in dipolar geometry. *J. Geophys. Res. Space Phys*. 2013, vol. 118, no. 4, pp. 1514–1528. DOI: 10.1002/jgra.50090.

Polyakov S.V., Rapoport V.O. The ionospheric Alfvén resonator. *Geomagnetism and Aeronomy*. 1981, vol. 21, pp. 816–822 (In Russian).

Singh A. K, Narayan D., Singh R.P. Propagation of extremely low frequency waves through the ionosphere. *Earth, Moon and Planets*. 2002, vol. 91, pp. 161–179. DOI: 10.1023/A:1022420426950.

Vavilov D.I., Shklyar D.R. Wave effects related to altitude variations in the ion composition of the ionosphere. *Radiophysics and Quantum Electronics*. 2016, vol. 59, no. 7. pp. 519–534. DOI: 10.1007/s11141-016-9720-8.

Whang Y. C. Attenuation of magnetohydrodynamic waves. *Astronomical J*. 1997, vol. 485, no.1 pp. 389–397.

Yeşil A., Sağir S. Updating conductivity tensor of cold and warm plasma for equatorial ionosphere F2-region in the Northern Hemisphere. *Iranian J. Science and Technology. Transaction A*. 2019, vol. 43, no. 5, pp. 315–320. DOI: 10.1007/s40995-017-0408-5.

URL: https://ccmc.gsfc.nasa.gov/modelweb/models/iri2016_vitmo.php (accessed December 14, 2022).

URL: https://ccmc.gsfc.nasa.gov/modelweb/models/msis_vitmo.php (accessed December 14, 2022).

URL:https://ccmc.gsfc.nasa.gov/modelweb/models/igrf_vitmo.php(accessed December 14, 2022).